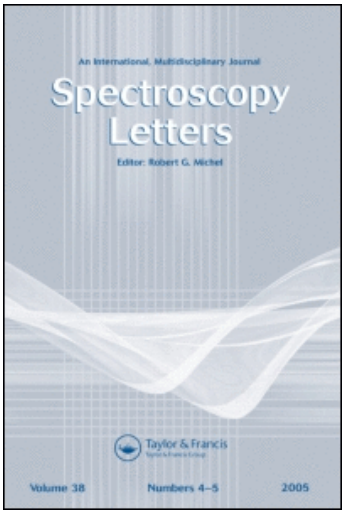

Spectroscopy Letters
Publication details, including instructions for authors and subscription information:
http://www.informaworld.com/smpp/title~content=t713597299

Microcolumn Electrophoresis for Electrokinetic Flow Analysis

Lian Li[a]; You-Zhao He[a]; Wu-Er Gan[a]
[a] Department of Chemistry, University of Science and Technology of China, Hefei, Anhui, People's Republic of China

Online publication date: 01 December 2009

To cite this Article Li, Lian , He, You-Zhao and Gan, Wu-Er(2009) 'Microcolumn Electrophoresis for Electrokinetic Flow Analysis', Spectroscopy Letters, 42: 6, 430 — 438
To link to this Article: DOI: 10.1080/00387010903187484
URL: http://dx.doi.org/10.1080/00387010903187484

Spectroscopy Letters, 42:430–438, 2009

ISSN: 0038-7010 print/1532-2289 online
DOI: 10.1080/00387010903187484

Taylor & Francis
Taylor & Francis Group

Microcolumn Electrophoresis for Electrokinetic Flow Analysis

Lian Li,
You-Zhao He,
and Wu-Er Gan

Department of Chemistry, University of Science and Technology of China, Hefei, Anhui, People's Republic of China

ABSTRACT A 2-mm i.d. and 100-mm length electrophoretic microcolumn packed with quartz microparticles was proposed in this article. To investigate the microcolumn preparation, thermal effect and electrophoretic separation, tryptophan and tyrosine were used as the target analytes, and their separation parameters were optimized, including quartz microparticle size, buffer concentration and pH, and so on. With the 2-mm i.d. fused-silica microcolumn packed with 9 μm length uniform quartz microncrystals and the electrophoretic buffer solution of 0.75 mmol/L sodium tetraborate (pH 11.0), the thermal effect of the microcolumn electrophoresis was limited satisfactorily, and underivatized tryptophan and tyrosine were separated on baseline and detected at 224 nm by an ordinary spectrophotometer. The limits of detection for tryptophan and tyrosine were 0.018 and 0.080 μmol/L, respectively. The separation efficiency of tryptophan was 4.0×10^4 plates/m. The sample capacity of the electrophoretic microcolumn achieved 35 μL. Owing to low consumption of reagent solutions and organic solvents, the microcolumn electrophoresis belongs to a green analytical method. With the advantages of high detection sensitivity, large sample capacity, instrumental simplicity, and portability, it can be employed as one of the high-performance separation techniques for an *in-situ* and real-time electrokinetic flow analysis system. It can also be developed for preparative electrophoresis.

KEYWORDS electrokinetic flow analysis, green analytical method, microcolumn electrophoresis, quartz microncrystals, quartz microparticles, thermal effect

An invited paper submitted to a special issue on Green Spectroscopy and Analytical Techniques, organized by Professor Miguel de la Guardia, of the Department of Chemistry, University of Valencia, Spain, and Professor Arabinda Kumar Das, of the Department of Chemistry, University of Burdwan, West Bengal, India.

Received 3 March 2009; accepted 3 March 2009.

Address correspondence to You-Zhao He, Department of Chemistry, University of Science and Technology of China, Hefei, Anhui 230026, People's Republic of China. E-mail: yzhe@ustc.edu.cn

INTRODUCTION

In chemical and biochemical analysis, the mature chromatography methods, including high performance liquid chromatography (HPLC), gas chromatography (GC), and so on, are used widely because of their high separation speed, detection sensitivity, and separation efficiency. But chromatographic apparatus are costly and complicated, and HPLC consumes large amounts of reagent solutions and organic solvents. Capillary electrophoresis (CE)[1] has been developed as a powerful separation technique with its advantages of high separation efficiency, fast analysis velocity, small sample/reagent consumption, multiform separation modes, and so on. But it also has its shortcomings, including limited sample capacity, restricted

concentration detectability, and so on, because of its small inner diameter. Without pre-concentration procedure and high sensitive detectors, such as mass spectrometry (MS) and laser-induced fluorescence (LIF) detector, the traditional CE is not suitable for the analysis of trace concentration samples, which are ubiquitous in our life, including contaminated environmental, food, and agricultural ones. To enhance the sample capacity and detection sensitivity, an electrophoretic microcolumn with millimeter diameter was studied for the trace concentration samples in our group.

Even if CE possesses high separation efficiency, its zone broadening should be controlled under well-selected conditions. Many fundamental works engaged in the zone broadening of CE. Remarkably, Knox and Grant[2] contributed the work on thermal effect of CE, and demonstrated that the thermal broadening of sample zones was proportional to the sixth power of the inner diameter of electrophoretic channel. Due to the electric current passed through electrophoretic channels, Joule heat is a ubiquitous phenomenon, and can seriously influence the electrophoretic separation, especially, with large diameter channel and high separation voltage. Thermal effect can increase the temperature in the electrophoretic channel, which may denature proteins, nucleic acids, and other live biological samples.[3] Furthermore, a significantly high temperature can generate vapor bubbles to disrupt the electrophoretic separation.[4] Thermal effect can enhance the radial temperature gradient and affect the temperature-related physicochemical parameters,[5,6] including dielectric constant, viscosity, electric conductivity, diffusion coefficient, pH value, and so on, and thus influence the electroosmotic flow (EOF),[7,8] and analyte electrophoresis.[9,10]

Therefore, the thermal effect is a difficult problem for an electrophoretic column with large inner diameter, in order to enhance sample capacity and improve detection sensitivity. In this article, 2 mm i.d. electrophoretic microcolumns were prepared by packing with quartz microparticles of different size and the thermal effect of the packed microcolumns was investigated. Tryptophan and tyrosine were used as the target analytes to evaluate the separation characteristic and thermal effect of the electrophoretic microcolumn. To diminish the thermal broadening, the separation parameters were optimized, including quartz microparticle size, buffer concentration, buffer pH, and so on. The proposed microcolumn electrophoresis was studied as one of the high-performance separation techniques for an electrokinetic flow analysis (EFA) system,[11] in which sample solutions are delivered by an electroosmotic pump,[12,13] treated by solid phase extraction,[14] and so on, separated by microcolumn electrophoresis, monolithic microcolumn electrochromatography,[15] or chromatography,[16] and detected by a fiber spectrophotometer.

Flow analysis techniques have contributed to achieving green analytical methods, by means of automation, miniaturization, and reducing reagent consumption and waste generation.[17] Comparing with flow injection analysis (FIA), sequential injection analysis (SIA)[18] not only can implement analytical functions without modification its manifold, but also limit its solvent and reagent consumption. Another simple, convenient, manageable, and low reagent consumption approach in flow analysis systems is multicommutation,[19,20] which consists of commutation devices, including solenoid valves and minipumps. Based on the flow analysis techniques mentioned earlier, the EFA system has been developed. Owing to the limited reagent and solvent consumption, and reduced waste generation, the microcolumn electrophoresis and EFA system can be employed as green analytical techniques.

EXPERIMENTAL

Apparatus

The electrophoretic microcolumn separation system, as shown in Fig. 1a, consisted of one laboratory-made electrophoretic microcolumn unit, one laboratory-made electroosmotic pump, two electrophoretic power supplies (DYY-12C, 10-5000 V and DYY-III-4, 20-1600 V, Liuyi Instrumental Factory, Beijing, China) providing the working voltages for electrophoretic separation and electroosmotic pump, respectively, one spectrophotometer (UV-9100, Rayleigh Analytical Instruments, Beijing, China), one three-way solenoid valve (161T031, Nreseach, Caldwell, NJ, USA) and one personal computer. Several microliter syringes (1–50 μL, Gaoge Instruments, Shanghai, China) of HPLC were adopted to inject sample solutions. The electrophoretic microcolumn unit was composed of one

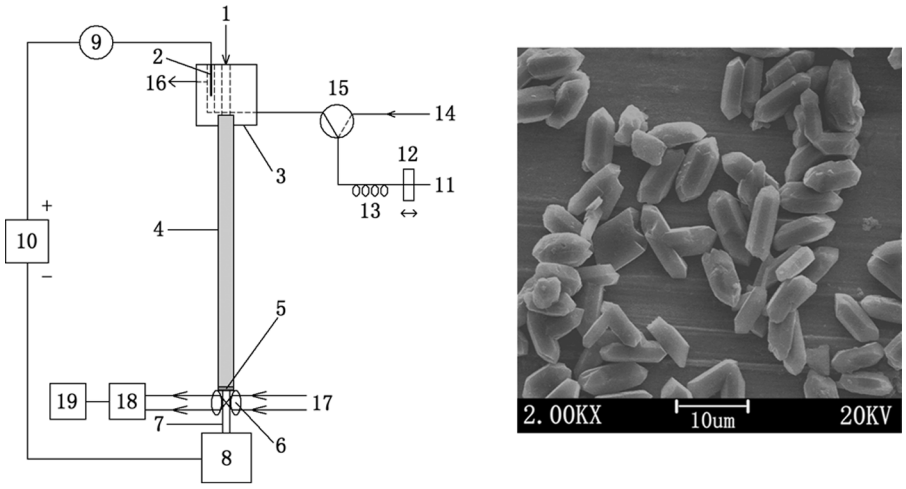

(a) (b)

FIGURE 1 **Schematic diagram of microcolumn electrophoresis system (a), (1) sample injection, (2) platinum electrode, (3) flow interface, (4) separation column, (5) nylon membrane, (6) quartz lens, (7) detection tube, (8) buffer reservoir, (9) milliampere meter, (10) electrophoretic power supply, (11) pump carrier, (12) electroosmotic pump, (13) holding coil, (14) running buffer, (15) solenoid valve, (16) waste, (17) incident light, (18) spectrophotometer, and (19) personal computer. And scanning electron micrograph of quartz microncrystals (b), the preparation conditions are 2.0 g silica gel mixed with 27 mL 0.46 mol/L KOH solution and synthesized at 350°C for 2 hr in an autoclave.**

100-mm length, 2-mm i.d., and 4-mm o.d. separation column jointed with a 20-mm length, 1.5-mm, i.d., and 3-mm o.d. detection tube by fritting and packed with quartz microncrystals, one on-column optical detector assembled with two 4-mm focus quartz lenses and their brass holders mounted to the detection tube, one PEEK flow interface jointed to the top of the electrophoretic microcolumn, and one buffer reservoir.

The sample solutions were injected on the top of the microcolumn through a lockable hole of the interface by a microliter syringe. The running buffer was aspirated and delivered by the electroosmotic pump at 2.0 mL/min (−500 V) and 0.1 mL/min (25 V), respectively, which showed less than 3.0 mL buffer solution was consumed for each sample analysis. The flow rate and direction of the pump were regulated by the supplied voltage and voltage polarity provided by the DYY-III-4 power supply. Both the pump and solenoid valve were controlled by the personal computer with a laboratory-made interface card and a Visual C program written by our group. The relative standard deviation (RSD) of the pump flow rate was 4.0%, measuring each 10 min for 4 hr. And the carrier solution inside the pump chambers should be replaced immediately after the pump finished the work.

A high temperature oven (SG2-3-10, 3 kW, 1000°C, Lixin Electric Apparatus Factory, Shanghai, China) was employed for hydrothermal synthesis. The crystalline phase of the quartz microncrystals was identified by an X-ray diffractometer (Philips X'Pert Pro Super, Amsterdam, The Netherlands) and their morphology was observed by a scanning electron microscope (KYKY 1010B, KYKY Technical Development, Beijing, China). The electric conductivity of solutions was determined by a conductometer (DDS-11A, Second Analytical Instruments, Shanghai, China). The zeta potential of quartz microncrystals in the running buffer was measured by a zetasizer (Nano ZS, Malvern Instruments, Worcestershire, UK). An ultrasonic cleaner (S-2200, 120 W, 35 KHz, J & L Technology, Shanghai, China) was used for degassing of the standard and buffer solutions.

Reagents and Solutions

Analytical-grade silica gels were obtained from Minuteness Nano-technology (Shanghai, China). Analytical-grade reagents of sodium tetraborate, hydrochloric acid, acetic acid, sodium acetate, sodium hydroxide, thiourea, tryptophan, and tyrosine were purchased from Sinopharm Chemical Reagent (Shanghai, China). All aqueous solutions were prepared with tri-distilled water (SZ-3, Huxi Analytical Instrument Factory, Shanghai, China).

1.25 mmol/L tryptophan and 2.5 mmol/L tyrosine stock solutions were prepared by dissolving the

reagents in distilled water and kept at 4°C. The mixed standard solution for electrophoresis separation was prepared by diluting the stock solutions with distilled water. The running buffer was 0.75 mmol/L sodium tetraborate buffer (pH 11.0). 0.5 mmol/L thiourea dissolved in the running buffer was used as the EOF marker. And the carrier solution of the electro-osmotic pump was 0.5 mmol/L hexamethylene tetramine.

Nylon membrane with 0.20 μm pore size was purchased from Millipore (Cork, Ireland). 2 mm i.d. and 1.5 mm i.d. fused-silica tubes were obtained from Lianyungang Dongxin Quartz Products (Jiangsu, China). Quartz microparticles were obtained from Lianyungang Huacheng Quartz Products (Jiangsu, China).

Electrophoretic Microcolumn Packed with Quartz Microparticles

Before packing quartz microparticles, the electrophoretic column was washed with 0.1 mol/L HCl, distilled water, 0.1 mol/L NaOH, and distilled water in turn, and dried at 60°C for 2 hr. 2 mmol/L sodium acetate (pH 3.0) was used as the packing buffer solution. Quartz microparticles were flushed with 0.01 mol/L HCl and distilled water, and soaked in the buffer solution for 6 hr. Then the electrophoretic microcolumn was clamped vertically, two pieces of nylon membrane were placed between the separation column and detection tube to hold the quartz microparticles inside the microcolumn. The slurry solution of quartz microparticles in the packing buffer was added into the separation column slowly by vibrating. When the whole microcolumn was filled with quartz microparticles, the microcolumn was packed by both the effects of EOF at 500 V and vibration on the side microcolumn. The quartz microparticles should be packed into the electrophoretic microcolumn carefully and homogeneously. Finally, the top of the microcolumn was sealed with a piece of nylon membrane and a nylon filter plate of 0.5 mm thickness.

Hydrothermal Synthesis of Uniform Quartz Microncrystals

Referring to the preparation of quartz nanocrystals,[21] the amorphous silica gel was used to prepare quartz microncrystals in a stainless steel autoclave with a 36-mL nickel inner lining by hydrothermal synthesis. The KOH solution was used to increase solubility of the silica gel as a mineralizer. 2.0 g dry silica gel was added into 27 mL 0.46 mol/L KOH solution and heated to 350°C at 10°C/min. After keeping the temperature at 350°C for 2 hr, the autoclave was cooled to room temperature. The products were washed with water and ethanol, and dried at 60°C for 4 hr. The crystalline phase was identified by the X-ray diffractometer with Cu Kα radiation ($\lambda = 1.54056$ Å) and the measuring conditions of 40 kV and 40 mA. The morphology was observed by the scanning electron microscope with a magnification of 2000, as shown in Fig. 1b. The average dimension of the quartz microncrystals was 9 μm × 4 μm.

Separation Procedure of Microcolumn Electrophoresis

Before the electrophoretic separation, the electrophoretic microcolumn was equilibrated with the running buffer. The standard and buffer solutions were degassed for 5 min by the ultrasonic cleaner. The mixed standard solutions were injected on the top of the electrophoretic microcolumn through the flow interface by a microlitre syringe quantitatively, separated at 800 V provided by the DYY-12C power supply, detected at 224 nm by the spectrophotometer and recorded by the personal computer. During the electrophoretic separation, a milliampere meter was employed to measure the electric current. The electrophoretic microcolumn was electrokinetically flushed with the running buffer for 5 min between the electrophoretic runs.

RESULTS AND DISCUSSION

Tryptophan and tyrosine can be detected by a UV-Vis spectrophotometer without derivatization and their isoelectric points (pI) are close to each other at 5.89 and 5.66, respectively. Therefore, the amino acids were chosen as the target analytes to evaluate the separation characteristic and thermal effect of the microcolumn electrophoresis.

Influence of Thermal Effect on Temperature-Dependent Parameters

Electrokinetic delivery is an efficient means to manipulate sample ions, buffer solution, and mobile phase in CE and capillary electrochromatography

(CEC). Compared with conventional pressure-driven flow, it has the significant advantages, such as plug-like flow and low backpressure. However, there exists inevitable Joule heat in separation channels, which increases the temperature and induces the radial temperature gradient in the separation microcolumn.

According to the heat balance equation, the radial temperature distribution inside a separation microcolumn can be expressed as[22]

$$T = T_1 + \frac{QR_1^2}{4\kappa_1}\left(1 - \frac{r^2}{R_1^2}\right) \quad (1)$$

where the variable r is radial position, T_1 is temperature of the microcolumn wall, R_1 is internal radius of the microcolumn, Q is heat generation per unit volume and κ_1 is thermal conductivity of buffer solution. The temperature gradient can influence the temperature-dependent parameters, including diffusion coefficient, electric conductivity, dynamic viscosity, dielectric constant, and so on.

The diffusion coefficient D_m of analytes can be given from the Stokes–Einstein equation[23]

$$D_m = \frac{k_B T}{6\pi\eta a} \quad (2)$$

where k_B is Boltzmann constant, η is dynamic viscosity of the solution, and a is radius of sample molecules. It manifests that temperature can affect diffusion coefficient proportionally.

Most of the studies assume that electric conductivity σ is a linear function of liquid temperature T[24]

$$\sigma = \sigma_0[1 + \alpha(T - T_0)] \quad (3)$$

where σ_0 is the electric conductivity at the room temperature T_0 and α is temperature coefficient.

For a dilute aqueous solution, its viscosity η and dielectric constant ε_r are close to those of pure water, and can be expressed as[4]

$$\eta = 2.761 \times 10^{-6} \exp(1713/T) \quad (4)$$

where η is in kg/ms and T in K, and

$$\varepsilon_r = 305.7 \exp(-T/219) \quad (5)$$

According to Eqs. (4) and (5), the viscosity and dielectric constant of the solution are the functions of the T-th root and the minus T-th power of constant e, respectively.

Effect of Quartz Microparticle Size on Thermal Effect

When electric current passes through a microcolumn, Joule heat is released and the buffer solution is heated. From the molecular movement theory, the frequent collisions between migrated ions and solvent molecules will convert part of the kinetic energy into heat in the microcolumn. The generated heat in the microcolumn is homogeneous, but the radial temperature distribution is paraboloidal because of the heat conduction through the microcolumn wall and surrounding air, as expressed in Eq. (1).

The released heat per unit volume of the buffer solution in a packed microcolumn is given as[2]

$$Q = E^2 \lambda c \varepsilon \quad (6)$$

where E is electric field strength, λ is molar conductivity, c is buffer concentration, and ε is porosity of the microcolumn. It indicates that Joule heat is proportional to microcolumn porosity.

With the determination method of Rathore and Horváth,[25] the porosity ε of the electrophoretic microcolumn packed with 9 μm length fine quartz microncrystals was about 40%. And packed with quartz microparticles from 45 μm to 360 μm, the porosity ε of electrophoretic microcolumn increased from 43% to 52%.

According to Ohm's law, the influence of electric field strength on electric current displays linearity under a constant conductivity of buffer solution. But the increased Joule heat can lead to a positive deviation of the Ohm's plots from its linearity, because the electric conductivity of buffer solution and the diffusion coefficient of electrolyte ions are enhanced by increasing the temperature. Therefore, a positive deviation of Ohm's plots implies that significant Joule heat has been generated in the microcolumn.

Fig. 2a showed the variation trend of electric current by increasing the electric field strength across the electrophoretic microcolumn packed with quartz microparticles from 9 to 360 μm. The positive deviation of electric current was observed by increasing the electric field strength and particle size, which led to increase the porosity. However, the electric current was linearly increased by the electric field

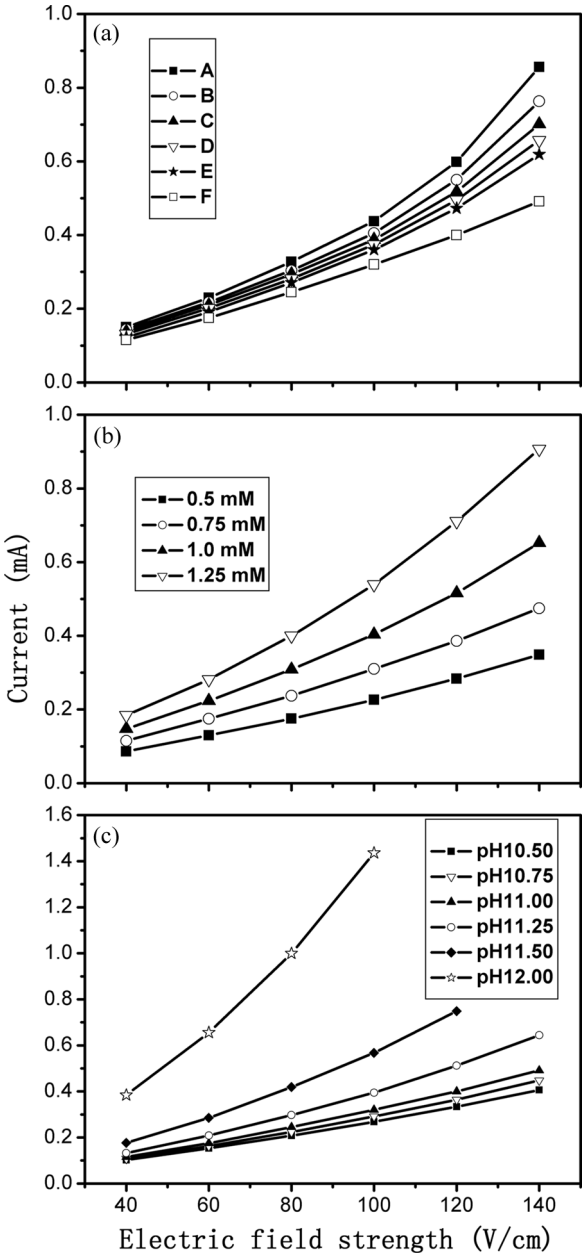

FIGURE 2 **Ohm's plots of electrophoretic microcolumn. (a) Effect of average size of packed quartz microparticle: A 360 μm, B 240 μm, C 150 μm, D 80 μm, E 45 μm, and F 9 μm, the buffer solution is 0.75 mmol/L sodium tetraborate (pH 11.0). (b) Effect of sodium tetraborate concentration, the average length of packed microncrystals is 9 μm and the buffer pH is 11.0. (c) Effect of buffer pH, the average length of packed microncrystals is 9 μm and the sodium tetraborate concentration is 0.75 mmol/L. The dimension of electrophoretic microcolumn is 2.0 mm I.D. × 10 cm length.**

strength up to 120 V/cm in the microcolumn packed with 9 μm quartz microncrystals. Therefore, 9 μm length quartz microncrystals prepared by hydrothermal synthesis could limit the thermal effect effectively and were packed in the electrophoretic microcolumn in this work.

The radial temperature gradient in the microcolumn can affect the plate height or plate number of the microcolumn. The plate height is significantly enhanced and the separation efficiency is seriously reduced in CE separation under a large temperature gradient. An equation for the plate height H_{TH} of thermal effect is expressed as[26]

$$H_{TH} = 10^{-8} \frac{\varepsilon_0 \varepsilon_r \zeta}{D_m \eta \kappa^2} E^5 d_c^6 \lambda^2 c^2 \varepsilon^2 \qquad (7)$$

where ε_0 is permittivity of vacuum, ζ is zeta potential, and d_c is microcolumn diameter. It indicates that the main parameters affecting the plate height H_{TH} are the microcolumn diameter, electric field strength, buffer concentration, molar conductivity, and microcolumn porosity.

In this work, the effect of quartz microparticle size on the separation efficiency of the electrophoretic microcolumn was examined in Table 1. The separation efficiencies of tryptophan were enhanced from 3.0×10^3 to 7.0×10^3 plates/m with the average microparticle size from 360 to 45 μm. Remarkably, the separation efficiency of tryptophan achieved 4.0×10^4 plates/m using the electrophoretic microcolumn packed with uniform 9 μm length quartz microncrystals,. It indicated that the separation efficiency increased rapidly when the quartz particle size decreased due to the decrease of the microcolumn porosity. These experimental data were accordant with the theoretical predictions in Eq. (7).

Effect of Support Buffer Concentration on Thermal Effect

From Eq. (6), we can find that buffer concentration has the obvious influence on Joule heat in the

TABLE 1 **Effect of Average Size of Quartz Microparticles on Separation Efficiency**[a]

Average size of quartz microparticles (μm)	360	240	150	80	45	9
Separation efficiency of tryptophan (plates/m)	3000	3790	4880	6080	7000	40,000

[a]The concentration of tryptophan and tyrosine are 0.125 mmol/L and 0.25 mmol/L. The injection volume is 1.0 μL, applied voltage is 800 V and detection wavelength is 224 nm, other conditions are the same as in Fig. 2a.

electrophoretic microcolumn, so it is an important parameter for the plate height of the electrophoretic microcolumn.

If H_{CES} is equal to the plate height of axial diffusion approximately, the following relation is supposed in Knox's work,[26]

$$H_{CES} > 10H_{TH} \tag{8}$$

From Eqs. (7) and (8), we obtain the limiting buffer concentration

$$c < 4500\frac{D_m\eta\kappa}{\varepsilon\lambda\varepsilon_0\varepsilon_r\zeta\, d_c^3E^3} \tag{9}$$

As in the aforementioned data, the porosity ε of the electrophoretic microcolumn packed with 9 μm length fine quartz microncrystals was about 40%. The molar conductivity λ of 0.048 $m^2/molΩ$ was measured by the conductometer. The zeta potential ζ of 36 mV was determined by the zetasizer. $\eta = 8.3\times10^{-4}$ kg/ms and $\varepsilon_r = 78$ were calculated by Eqs. (4) and (5) with $T = 300$ K, respectively. The permittivity of vacuum ε_0 was the constant of 8.85×10^{-12} C^2/Nm^2. The values of $D_m = 1.0\times10^{-9}$ m^2/s and $\kappa = 0.6$ W/mK were adopted as those in Knox's work.[26] Under our experimental conditions, d_c and E were 2.0×10^{-3} m and 8.0×10^3 V/m (viz., 80 V/cm), respectively. By substituting the aforementioned data into Eq. (9), the electrolyte concentration of the running buffer should be lower than 1.1 mmol/L.

By increasing the buffer concentration and the electric field strength, the effects of Joule heat were illustrated in Fig. 2b. It displayed the variation of the electric current with the field strength from 20 to 140 V/cm and buffer concentrations of 0.50, 0.75, 1.0, and 1.25 mmol/L sodium tetraborate (pH 11.0). It was found that the positive deviation of the electric current was observed with the sodium tetraborate concentration and electric field strength higher than 1.0 mmol/L and 80 V/cm. Contrarily, with the buffer concentration lower than 0.75 mmol/L, the linearity of the electric current could be retained by increasing the electric field strength to 120 V/m.

Therefore, to obtain adaptive buffer capacity, high separation efficiency, and fast separation speed, and avoid excessive Joule heat, the tetraborate concentration and electric field strength were selected at 0.75 mmol/L and 80 V/cm in this work.

Effect of Support Buffer pH on Thermal Effect

The pH value of running buffer is one of the important parameters for the electrophoretic separation. Electrophoretic mobility is directly related to the mass and charge of the analytes and EOF is affected by the surface charge density of the packed quartz microparticles and separation column. It implies that both the electrokinetic phenomena are dependent on the pH value of the running buffer.

In this work, the effect of buffer pH on the analyte separation was examined from pH 10.5 to 12.0. As shown in Fig. 2c, the positive deviations of electric current were observed with the pH value higher than 11.0, which resulted from the high concentration of NaOH introduced into the buffer solution to obtain high pH value.

Moreover, the effect of buffer pH on the resolution of tryptophan and tyrosine is presented in Table 2. It was found that the resolutions of tryptophan and tyrosine increased with the pH value from 10.5 to 11.0, and then retained almost constant with the buffer solution higher than pH 11.0. According to the experimental results, the migration time of the amino acids was prolonged by increasing the buffer pH. The reduced apparent velocities of the analytes implied that the velocity of EOF decreased, because the migrating direction of EOF was opposite to those of the amino acid anions in the basic buffer solution. To obtain the pH value from pH 11.0 to 12.0, the ionic strength of the running buffer was enhanced obviously by introducing large amount of NaOH. Based on the relation between the electrophoretic resolution and diffusion coefficient, resultant mobility of EOF and analytes,[1] the reduction of the diffusion coefficient and resultant velocity from pH 10.5 to 11.0 could enhance the resolution. However, the high ionic strength of the buffer solution and thermal effect led to the resolution retained at about 1.74

TABLE 2 Resolution of Tryptophan and Tyrosine with Different Buffer pH[a]

Buffer pH	10.5	10.75	11.0	11.25	11.5	12.0
Resolution	1.68	1.72	1.74	1.73	1.73	1.74

[a]9 μm quartz microncrystals packed into the electrophoretic microcolumn are prepared by hydrothermal synthesis, other conditions are the same as in Table 1.

with the buffer pH higher than 11.0. So, the recommended pH value of the running buffer was chosen at 11.0.

Electrophoretic Separation by the Microcolumn Packed with Uniform Quartz Microncrystals

The electrophoretic separation of tryptophan and tyrosine was carried out with 0.75 mmol/L sodium tetraborate (pH 11.0) running buffer by the electrophoretic microcolumn packed with 9 μm length quartz microncrystals. The electropherogram is illustrated in Fig. 3. It was found that two amino acids were separated on baseline and their peaks were symmetrical. The separation efficiency of tryptophan and tyrosine were 4.0×10^4 and 3.2×10^4 plates/m, respectively. The experimental results implied that the electrophoretic microcolumn packed with 9 μm uniform quartz microncrystals prepared by hydrothermal synthesis could obtain the satisfactory separation efficiency.

The precisions or relative standard deviations (RSDs) of retention time for tryptophan and tyrosine were 0.39% and 0.18%, and those of peak height were 3.2% and 4.5%, respectively, which were obtained by five individual runs with the same electrophoretic microcolumn and separation conditions.

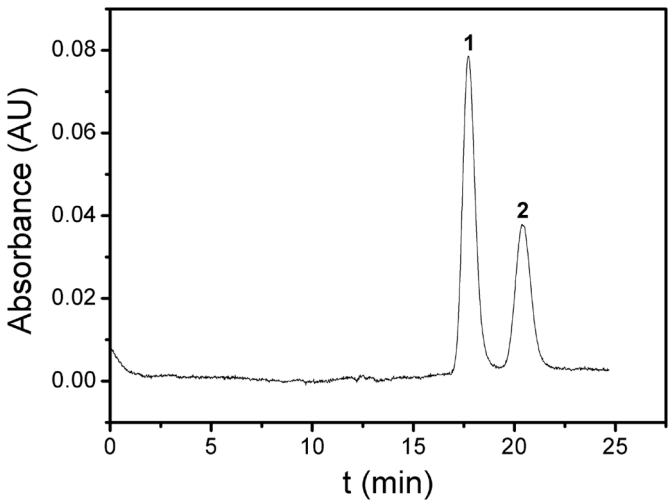

FIGURE 3 **Electropherogram of tryptophan (1) and tyrosine (2) by the electrophoretic microcolumn packed with 9 μm length uniform quartz microncrystals. The concentration of tryptophan and tyrosine are 0.125 mmol/L and 0.25 mmol/L. The injection volume is 1.0 μL, applied voltage is 800 V, and detection wavelength is 224 nm. Other conditions are the same as in Fig. 2a.**

It indicated that the reproducibility and reliability of the electrophoretic microcolumn were satisfied.

Based on the chromatographic definition, the sample capacity of the electrophoretic microcolumn was calculated to be about 35 μL after surveyed the peak widths by increasing the sample volume up to 40 μL. It was much higher than that of CE, so the detection sensitivity of the microcolumn electrophoresis could be improved.

When the sample volume was 30 μL and the concentrations of amino acids were in the range of 0.2–8.0 μmol/L, the detection limits of detection (LODs, S/N = 3) of tryptophan and tyrosine were 0.018 and 0.080 μmol/L, respectively. The LODs of the microcolumn electrophoresis obtained by a commercial UV-Vis spectrophotometer and without troublesome derivatization were close to laser-induced fluorescence detection of CE and better than mass spectrometric and derivatized UV-Vis spectrometric detection of CE.[27–29] Therefore, the microcolumn electrophoresis can be employed in the analysis of large amount and low concentration samples without pre-concentration, such as environmental, food, and agricultural samples. It can also be developed for preparative electrophoresis. Compared with HPLC, the LODs of the microcolumn electrophoresis with underivatized UV detection were better than those of derivatized UV-Vis detection, but worse than fluorescence detection of HPLC.[30,31]

With the merits of equipment simpleness and portability, detection sensitivity, sample capacity, and environment friendliness, the proposed electrophoresis technique can be employed as one of the high-performance separation techniques of the EFA system for *in-situ* and real-time environment analysis.

ACKNOWLEDGEMENT

The authors gratefully thank the Natural Science Foundation of China (No. 20675075) for the financial support to carry out this work.

REFERENCES

1. Jorgenson, J. W.; Lukacs, K. D. Zone electrophoresis in open-tubular glass capillaries. *Anal. Chem.* **1981**, *53*, 1298–1302.
2. Knox, J. H.; Grant, I. W. Miniaturisation in pressure and electroendosmotically driven liquid chromatography: Some theoretical considerations. *Chromatographia* **1987**, *24*, 135–143.
3. Rush, R. S.; Cohen, A. S.; Karger, B. L. Influence of column temperature on the electrophoretic behavior of myoglobin and a-lactalbumin

in high-performance capillary electrophoresis. *Anal. Chem.* **1991**, *63*, 1346–1350.
4. Knox, J. H.; McCormack, K. A. Temperature effects in capillary electrophoresis. 1: Internal capillary temperature and effect upon performance. *Chromatographia* **1994**, *38*, 207–214.
5. Xuan, X. C. Joule heating in electrokinetic flow. *Electrophoresis* **2008**, *298*, 33–43.
6. Cetin, B.; Li, D. Q. Effect of Joule heating on electrokinetic transport. *Electrophoresis* **2008**, *29*, 994–1005.
7. Maynes, D.; Webb, B. W. The effect of viscous dissipation in thermally fully-developed electro-osmotic heat transfer in microchannels. *Int. J. Heat Mass Transfer* **2004**, *47*, 987–999.
8. Horiuchi, K.; Dutta, P. Joule heating effects in electroosmotically driven microchannel flows. *Int. J. Heat Mass Transfer* **2004**, *47*, 3085–3095.
9. Tang, G. Y.; Yan, D. G.; Yang, C.; Gong, H. Q.; Chai, J. C.; Lam, Y. C. Assessment of Joule heating and its effects on electroosmotic flow and electrophoretic transport of solutes in microfluidic channels. *Electrophoresis* **2006**, *27*, 628–639.
10. Chein, R.; Yang, Y. C.; Lin, Y. S. Estimation of Joule heating effect on temperature and pressure distribution in electrokinetic-driven microchannel flows. *Electrophoresis* **2006**, *27*, 640–649.
11. He, Y. Z.; Wang, X. K.; Deng, N.; Wang, L.; Han, F. Electrokinetic Flow Total Analysis System. *Chinese Patent* **2008**, ZL 200510038677.5.
12. He, Y. Z.; Gan, W. E.; Zhang, M.; Zheng, M. Z. Determination of fluoride in tap water with electroosmosis pump flow injection-spectrophotometry. *Chin. J. Anal. Chem.* **1998**, *26*(2), 125–128.
13. Gan, W. E.; Yang, L.; He, Y. Z.; Zeng, R. H.; Cervera, M. L.; de la Guardia, M. Mechanism of porous core electroosmotic pump flow injection system and its application to determination of chromium (VI) in waste-water. *Talanta* **2000**, *51*(4), 667–675.
14. Han, F.; He, Y. Z.; Li, L.; Fu, G. N.; Xie, H. Y.; Gan, W. E. Determination of benzoic acid and sorbic acid in food products using electrokinetic flow analysis–ion pair solid phase extraction–capillary zone electrophoresis. *Anal. Chim. Acta* **2008**, *618*, 79–85.
15. Deng, N.; He, Y. Z.; Wang, L.; Wang, X. K.; Su, Q. D. Reversed-phase electrochromatography with a monolithic microcolumn prepared in a 2.2-mm-inner diameter fused-silica tube. *Anal. Chem.* **2005**, *77*(17), 5622–5627.
16. Wang, L.; He, Y. Z.; Deng, N.; Wang, X. K.; Fu, G. N. Reversed-phase liquid chromatography with electrokinetic flow analysis system. *Instrum. Sci. Technol.* **2006**, *34*, 743–753.
17. de la Guardia, M.; Ruzicka, J. Towards environmentally conscientious analytical chemistry through miniaturization, containment and reagent replacement. *Analyst* **1995**, *120*, 17N.
18. Ruzicka, J.; Marshall, G. D. Sequential injection: A new concept for chemical sensors, process analysis and laboratory assays. *Anal. Chem. Acta* **1990**, *237*, 329–343.
19. Reis, B. F.; Gine, M. F.; Zagatto, E. A. G.; Lima, J. L. F. C.; Lapa, R. A. Multicommutation in flow analysis. Part 1. Binary sampling: concepts, instrumentation and spectrophotometric determination of iron in plant digests. *Anal. Chem. Acta* **1994**, *293*(1–2), 129–138.
20. Reis, B. F.; Morales-Rubio, A.; de la Guardia, M. Environmentally friendly analytical chemistry through automation: Comparative study of strategies for carbaryl determination with *p*-aminophenol. *Anal. Chim. Acta* **1999**, *392*(2–3), 265–272.
21. Yanagisawa, K.; Zhu, Y.; Onda, A.; Kajiyoshi, K. Hydrothermal synthesis of mono-dispersed quartz powders. *J. Mater. Sci.* **2004**, *39*, 2931–2934.
22. Grushka, E.; McCormick, R. M.; Kirkland, J. J. Effect of temperature gradients on the efficiency of capillary zone electrophoresis separations. *Anal. Chem.* **1989**, *61*, 241–246.
23. Masliyah, J. H. *Electrokinetic Transport Phenomena*; Alberta Department of Energy. Press: Edmonton, 1994.
24. Gobie, W. A.; Ivory, C. F. Thermal model of capillary electrophoresis and a method for counteracting thermal band broadening. *J. Chromatogr.* **1990**, *516*, 191–210.
25. Rathore, A. S.; Horváth, Cs. Axial nonuniformities and flow in columns for capillary electrochromatography. *Anal. Chem.* **1998**, *70*, 3069–3077.
26. Knox, J. H. Thermal effects and band spreading in capillary electro-separation. *Chromatographia* **1988**, *26*, 329–337.
27. Thongkhao-On, K.; Kottegoda, S.; Pulido, J. S.; Shippy, S. A. Determination of amino acids in rat vitreous perfusates by capillary electrophoresis. *Electrophoresis* **2004**, *25*, 2978–2984.
28. Soga, T.; Kakazu, Y.; Robert, M.; Tomita, M.; Nishioka, T. Qualitative and quantitative analysis of amino acids by capillary electrophoresis-electrospray ionization-tandem mass spectrometry. *Electrophoresis* **2004**, *25*, 1964–1972.
29. Komarova, N. V.; Kamentsev, J. S.; Solomonova, A. P.; Anufrieva, R. M. Determination of amino acids in fodders and raw materials using capillary zone electrophoresis. *J. Chromatogr. B* **2004**, *800*, 135–143.
30. Gómez-Alonso, S.; Hermosín-Gutiérrez, I.; García-Romero, E. Simultaneous HPLC analysis of biogenic amines, amino acids, and ammonium ion as aminoenone derivatives in wine and beer samples. *J. Agric. Food Chem.* **2007**, *55*, 608–613.
31. Bosch, L.; Alegría, A.; Farré, R. Application of the 6-aminoquinolyl-*N*-hydroxysccinimidyl carbamate (AQC) reagent to the RP-HPLC determination of amino acids in infant foods. *J. Chromatogr. B* **2006**, *831*, 176–183.